# Monte Carlo Simulations of β-Hairpin Folding at Constant Temperature

Shen-Shu Sung
The Lerner Research Institute, The Cleveland Clinic Foundation, Cleveland, Ohio 44195 USA

ABSTRACT Monte Carlo simulations were applied to β-hairpin folding of a valine-based peptide. Two valine residues in the middle of the peptide were substituted with glycine, to serve as turn residues. Unlike lattice model simulations, structure prediction methods, and unfolding simulations, our simulations used an atom-based model, constant temperature (274 K), and non-β-hairpin initial conformations. Based on the concept of solvent reference, the effective energy function simplified the solvent calculation and overcame the multiple minima problem. Driven by the hydrophobic interaction, the peptide first folded into a compact U-shaped conformation with a central turn, in analogy to the initial collapse with simultaneous nucleation in protein folding. The peptide units in the U-shaped conformation then reoriented, gradually forming hydrogen bonds in the β-hairpin pattern from the β-turn to the ends of the strands. With the same energy function, an alanine-based peptide folded into helix-dominated structures. The basic structure types (α-helix or β-hairpin) that formed during the simulations depended upon the amino acid sequence. Compared with helix, β-hairpin folding is driven mainly by the hydrophobic interaction. Hydrogen bonding is necessary to maintain the ordered secondary structure.

## INTRODUCTION

Molecular simulation is a direct computational approach to studying structural changes in a wide range of physical and biological problems. However, direct simulation of protein folding at the atomic level has not been possible because of the folding time scale and the number of degrees of freedom in a protein-solvent system. Consequently, folding has been studied using other methods. Lattice models, which neglect some atomic details, have been used in developing folding theories (Taketomi et al., 1975; Dill 1985; Skolnick and Kolinski, 1990; Shakhnovich and Gutin, 1991). The energy minimization, the simulated annealing, and other related methods have been used to study peptide structures (Ripoll and Scheraga, 1988; Okamoto et al., 1991). Recently, constant temperature molecular simulations of peptide folding have been reported using implicit solvent models (Sung, 1994, 1995; Sung and Wu, 1996, 1997) and explicit solvent models (Daura et al. 1998).

To simulate folding at constant temperature, two approaches have been tested: using a detailed representation of the protein-solvent system in short-time simulations, or using longer-time simulations with a simplified system. The former is a widely accepted approach. But, in most cases, it can only start with the native structure of a protein, such as the unfolding simulations. Currently, it is not yet clear to what extent, or on what issue, the unfolding simulations with higher temperature represent the reversal of folding (Finkelstein 1997). For folding simulations, the continuum solvent approach is still worth investigating (Schaefer and Karplus, 1995; Okamoto, 1998). As an approximation, one may assume that the solvent effect can be separated into two parts: the average effect (which does not depend on specific solvent configurations) and the specific interaction, such as solvent-protein hydrogen bonding. This hypothesis can be tested computationally to see whether the continuum solvent approach can study the aspect of structural changes resulting from the average solvent effect. The key issue is to find an appropriate effective energy function. The current study focuses on testing effective energy functions on β-hairpin folding.

Compared with helix studies, similar experimental data related to monomeric β-sheet or β-hairpin formation are scarce. The search for models of β-sheet or β-hairpin formation led to peptides containing non-natural amino acids at the turn region or to nonpeptide scaffolds that bring the β-strands together. Examples of linear peptides that contain only natural L-amino acids in their sequence and that fold into monomeric β-hairpin conformations in aqueous solution have been only recently reported. Apart from the one described by Blanco et al. (1994), which is a fragment of a native protein, the others are designed peptides (Alba et al., 1995, 1997; Blanco et al., 1993; Ramirez-Alvarado et al., 1996). These peptides show partial β-hairpin conformation (less than 50%), which is in equilibrium with coil conformations. Very recently, triple-strand β-sheets have been successfully synthesized (Schenck and Gellman, 1998; Kortemme et al., 1998).

Computationally, the empirical force fields have great difficulty in simulating folding of the β-sheet. To our knowledge, there has not been a simulation of folding of the β-sheet at the atomic level. In our previous work, we simulated the helix folding of alanine-based peptides using both the Monte Carlo (MC) method (Sung, 1994, 1995) and molecular dynamics (MD) simulations (Sung and Wu, 1996, 1997) at a constant temperature (274 K). In the current study, we focus on the folding simulation of a simple β-hairpin structure. Just as polyalanine was used as

*Received for publication 16 June 1998 and in final form 7 October 1998.*
Address reprint requests to Dr. Shen-Shu Sung, The Lerner Research Institute, FF3, Cleveland Clinic Foundation, 9500 Euclid Avenue, Cleveland, OH 44195. Tel.: 216-444-0056; Fax: 216-444-9263; E-mail: sungs@cesmpt.ccf.org.

0006-3495/99/01/164/12 $2.00

a theoretical model for helix simulations (Ripoll and Scheraga, 1988; Daggett and Levitt, 1992), a valine-based model peptide with two glycine residues at the turn is used for the β-hairpin folding.

## MODEL AND METHODS

The model and methods have been described previously (Sung, 1994, 1995). Here, we briefly mention the basic principles and describe the new features. The basic idea underlying the model is to use an average solvent effect as the reference in energy functions to simplify the solvent calculation. The solvent effect is a function of many variables, such as solvent configurations. An average effect is a first approximation. For example, continuum solvent models use the average effect over the solvent configurations. The solvent-referenced potential may also reduce the inaccuracy caused by the cancellation of large energy terms calculated with vacuum reference. The in vacuo calculations overestimate the energy changes that occur upon conformational changes (Daggett et al., 1991). The competing effects of the solvent, such as the van der Waals (VDW) attraction and hydrogen bonding between the protein and solvent, reduce the strength of the interactions and consequently reduce the energy barrier related to the multiple minima problem.

### VDW interactions

In solution, the intramolecular VDW interactions of a protein molecule are balanced by the intermolecular VDW interactions with solvent molecules. Thus, when solvent molecules are not explicitly included, the intramolecular VDW interactions must be adjusted accordingly. The longer-range attractive VDW interactions provide a nearly uniform background potential (Chandler et al., 1983) and therefore can serve as the reference for the VDW energy calculation (McCammon et al., 1980). The possible difference between the protein intramolecular VDW attraction and that with water may be included in the hydrophobic interaction energy. The short-range repulsion represents the exclusive volume of each atom and needs to be calculated explicitly. Based on this consideration, we apply a shifted truncation to the VDW interaction, as shown in Eq. 1, where $r$ is the distance between two interacting atoms and $r^*$ is the minimal energy distance for the given pair of atoms. To compensate for thermal motion, $r^*$ is scaled to 95% of the original value of the AMBER force field (Weiner et al., 1984):

$$E_{\mathrm{VDW}}(r) = \begin{cases} \epsilon\left[\left(\dfrac{r^*}{r}\right)^{12} - 2\left(\dfrac{r^*}{r}\right)^{6} + 1\right] & r < r^* \\ 0 & r \geq r^* \end{cases} \quad (1)$$

### Dielectric constant

To include the dielectric screening effect of the solvent, the dielectric constant needs to be adjusted. Both constant and distance-dependent dielectric functions have been suggested for the AMBER force field (Weiner et al., 1984; Daggett et al., 1991). In our previous work on helix folding simulations, distance-dependent dielectric functions have been tested. In the current study, different constants, 1, 2, 3, and 4, were tested with the AMBER parameters of the atomic partial charges (Weiner et al., 1984). In most simulations, dielectric constant 2 has been used, because dielectric constant 1 overestimates the Coulomb interaction in a calculation without water (Daggett et al., 1991), and dielectric constants 3 and 4 may make hydrogen bonds unstable. Dielectric constant 2 has been used previously with a different force field (Momany et al., 1975) and different calculation methods, such as the electrostatic hydration calculation (Yang and Honig, 1995). The concept of the dielectric constant was originally proposed for a continuum. In molecular simulations, it may be treated as a scaling factor for a specific type of system, rather than an exact physical quantity (Finkelstein, 1997).

### Hydrophobic effect

The important hydrophobic effect is often assumed to be proportional to the solvent-accessible surface area (Eisenberg and McLachlan, 1986; Ooi and Oobatake, 1991). Computationally, the solvent-accessible surface area calculation is simpler than including thousands of water molecules, but it still increases the computing time by ~15-fold compared with that without this calculation. As an approximate method based on average effects, the accurate surface area calculation may not be absolutely necessary in all cases. Kurochkina and Lee (1995) have shown that the pairwise sum of the buried surface area is linearly related to the true buried area, as calculated by the algorithm of Lee and Richards (1971), and to the contact potential of Miyazawa and Jernigan (1985). Therefore, in the current study, we chose a simple pairwise interaction model, based on the idea of Kurochkina and Lee (1995). Instead of using a scaling factor, an average surface area buried by a contacting atom is used in our study. The pairwise interaction of the hydrophobic effect is often used in lattice models (Skolnick and Kolinski, 1990; Dill et al., 1995). The success of the lattice model in developing folding theories may provide some justification for this approximation in qualitative folding studies.

The average area buried by a contacting water molecule is ~9.6 Å$^2$, and the average area buried by a contacting carbon atom is ~⅓ of that by water (Colonna-Cesari and Sander, 1990). For the sake of simplicity, a buried area of 3.2 Å$^2$ was used for all nonhydrogen atoms in our calculation. The hydrogen atoms are treated as part of the atoms to which they are covalently bonded. Different values of the average buried area were tested in combination with the solvation parameters, as mentioned in the following paragraphs. As the two atoms move apart, the interaction energy decreases linearly, and as they move 2.8 Å (the diameter of a water molecule, as used in most surface area calculations) beyond their VDW contact, the interaction becomes zero. In the current study, the hydrophobic interaction free energy $\Delta G$ is the sum of the contribution from each atom pair $\Delta G_{ij}$, which is calculated according to Eq. 2:

$$\Delta G_{ij} = -A(\Delta\sigma_i f(r) + \Delta\sigma_j f(r)), \quad (2)$$

with

$$f(r) = \begin{cases} 0 & \text{for } r > r^* + R \\ (r^* + R - r)/R & \text{for } r^* \leq r \leq r^* + R \\ 1 & \text{for } r < r^* \end{cases},$$

where $\Delta\sigma_i$ and $\Delta\sigma_j$ are the solvation parameters of the two interacting atoms, $A$ is the average buried area (3.2 Å$^2$ in most tests), $r^*$ and $r$ are the same as in Eq. 1, and $R$ is the interaction range (2.8 Å in most tests) beyond $r^*$. Because $A$ is the buried area, instead of the solvent-accessible area, a negative sign is needed in Eq. 2.

The exact value of $\Delta\sigma$ is under intense debate. The early estimate was ~25 cal/mol/Å$^2$ for the hydrophobic surface of proteins (Chothia, 1974). Sharp et al. (1991) proposed a larger value of ~47 cal/mol/Å$^2$. For our study, the most important question is what value is compatible with the parameters used for the atomic partial charges and the VDW interaction. In our previous study (Sung and Wu, 1996), the $\Delta\sigma$ values used for C and O atoms were 25.8 and −25.1 cal/mol/Å$^2$, respectively. In the current study, a single value with opposite signs for the hydrophobic and hydrophilic groups, ±25 cal/mol/Å$^2$, was tested to keep the number of parameters as small as possible. For hydrophobic atoms, including all carbon atoms, the sign is positive. For hydrophilic atoms, including O and N, the sign is negative. The $N^+$ and $O^-$ atom types were not encountered in this study. Other values of $\Delta\sigma$, ±35 cal/mol/Å$^2$, ±47 cal/mol/Å$^2$, and 0, have also been tested, and the results are presented in the following section. With a single value of the solvation parameter (e.g., 25 cal/mol/Å$^2$), the value of $\Delta\sigma$ in Eq. 2 may be combined with the value of the surface area $A$ (e.g., 3.2 Å$^2$) to form a single parameter or scaling factor (e.g., 80 cal/mol), rather

than being considered as accurate physical properties, because both the surface area assumption and the value of the solvation free energy are approximate. Therefore, the parameters of $\pm 35$ cal/mol/Å$^2$ and 3.2 Å$^2$ are equivalent to $\pm 25$ cal/mol/Å$^2$ and 4.5 Å$^2$; the parameters of $\pm 47$ cal/mol/Å$^2$ and 3.2 Å$^2$ are equivalent to $\pm 25$ cal/mol/Å$^2$ and 6.0 Å$^2$ or to $\pm 35$ cal/mol/Å$^2$ and 4.3 Å$^2$. The test on solvation parameters will also serve as a test on different average surface areas.

In the current study, the hydrophilic interaction, including electrostatic hydration, is treated as a negative hydrophobic effect within the framework of the surface-area-based approximation. However, the electrostatic hydration has an interaction range longer than the first layer of water. To see the effect of different interaction ranges, the interaction range $R = 2.8$ Å in Eq. 2 could be increased to include the interactions beyond the first layer of water molecules. An interaction range of $R = 5.6$ Å has been tested, and the results are reported in the next section.

Gilson and Honig (1991) proposed a simple model for electrostatic hydration for molecular simulations, as a function of the interatomic distance $r^{-4}$. This distance dependence with an interaction range of 15 Å has been tested for the hydrophilic atoms O and N, and shown in Eq. 3, assuming the same energy at $r^*$ as in the linear distance dependence. For hydrophobic atoms ($\Delta\sigma > 0$), the formula for $f(r)$ in Eq. 2 is used:

$$\Delta G_{ij} = -A(\Delta\sigma_i F_i(r) + \Delta\sigma_j F_j(r)) \quad (3)$$

with

$$F_i(r) = r^{*4}/r^4 \quad \text{for } \Delta\sigma_i < 0$$
$$F_i(r) = f(r) \quad \text{for } \Delta\sigma_i > 0$$
$$F_j(r) = r^{*4}/r^4 \quad \text{for } \Delta\sigma_j < 0$$
$$F_j(r) = f(r) \quad \text{for } \Delta\sigma_j > 0$$

## The Monte Carlo method

The MC simulations were carried out using the rigid element algorithm we developed previously (Sung, 1994, 1995). The -CONH- units were treated as rigid elements connected to $C_\alpha$ atoms by flexible bond lengths and angles to allow independent local motions of the backbone. Unlike our previous model, in the current study all the nonhydrogen atoms of the side chains are explicitly represented. Side chain motions are represented by single bond rotations, which is efficient for short chains. The calculations were carried out on SGI Indigo workstations.

## The model peptide

Just as polyalanine has been widely used for helix folding simulations without considering the practical aggregation problem (Ripoll and Scheraga, 1988; Daggett and Levitt, 1992), the valine-based peptide Ac-VVVVVGGVVVVV-$NH_2$ was used as a theoretical model for $\beta$-hairpin folding because valine has consistently shown a low helical tendency and a high $\beta$-sheet tendency in many previous studies (Chou and Fasman, 1973, 1974; Wojcik et al., 1990; Chakrabartty et al., 1994). The glycine residues in the center were designed to form the two-residue $\beta$-turn because the glycine backbone is very flexible. A shorter sequence, Ac-VVVVGGVVVV-$NH_2$, was also tested. Like polyalanine, this valine-glycine peptide is a theoretical model. Experimentally, aggregation will be a problem for this peptide. Charged or polar residues are needed to make it soluble in water. The site of the insertion (or substitution) and the type of the amino acid have to be carefully designed and tested. To see the sequence dependence of folding, a helix-forming alanine-based synthetic peptide, Ac-$(AAQAA)_3$Y-$NH_2$, was simulated with the same energy function. Experimentally, its helical content is ~50%, measured by circular dichroism (Scholtz et al., 1991). All our simulations were conducted using the MC method at a constant temperature of 274 K, because the experimental measurements of some of those synthetic peptides were carried out at this temperature.

# RESULTS AND DISCUSSION

## Extended initial conformation

Several simulations were carried out, as listed in Table 1. The first simulation was for the peptide Ac-VVVVVGGV-VVVV-$NH_2$ with dielectric constant 2 and atomic solvation parameter $\pm 25$ cal/mol/Å$^2$ (simulation 1 in the Table 1). The initial conformation was fully extended. The conformations at steps 9 million (M), 45 M, 86 M, and 200 M during the MC simulation are shown in Fig. 1. As the simulation started, the structure relaxed into various coil

**TABLE 1 Summary of various simulation parameters and results**

| Simulation | Initial conformation | Solvation* | Dielectric constant | Stable conformation |
|---|---|---|---|---|
| 1 | Ext. | ±25/2.8 | 2 | $\beta$-Hairpin |
| 2 | **Helix** | ±25/2.8 | 2 | $\beta$-Hairpin |
| 3 | Ext. | **±35**/2.8 | 2 | $\beta$-Hairpin |
| 4 | **Helix** | **±35**/2.8 | 2 | $\beta$-Hairpin |
| 5 | Ext. | **±47**/2.8 | 2 | Compact |
| 6 | Ext. | **0**/2.8 | 2 | Unstable |
| 7 | Ext. | ±25/**5.6** | 2 | $\beta$-Hairpin |
| 8 | Ext. | ±25/**15**[#] | 2 | $\beta$-Hairpin |
| 9 | Ext. | ±25/2.8 | 3 | $\beta$-Hairpin[§] |
| 10 | Ext. | ±25/2.8 | 4 | Unstable |
| 11 | Ext./$\alpha$/$\beta$[¶] | ±25/2.8 | 1 | Compact/$\alpha$/$\beta$[‖] |
| 12 **$(AAQAA)_3$Y** | Ext. | ±25/2.8 | 2 | Helix |

Compared with simulation 1, the different parameters tested are shown in bold. Except simulation 12, which is carried out on the alanine-based peptide, all other simulations (1–11) are on the valine-based peptide.

*This column contains the solvation parameter in cal/mol/Å$^2$ and the solvation interaction range in Å.

[#]The $r^{-4}$ distance dependence was used for O and N atoms.

[§]The $\beta$-hairpins were short and the conformations changed more frequently.

[¶]This row included three simulations with different initial conformations: Ext., extended; $\alpha$, $\alpha$-helix; $\beta$; $\beta$-hairpin.

[‖]The stable structure depends on the initial conformation. See text for details.

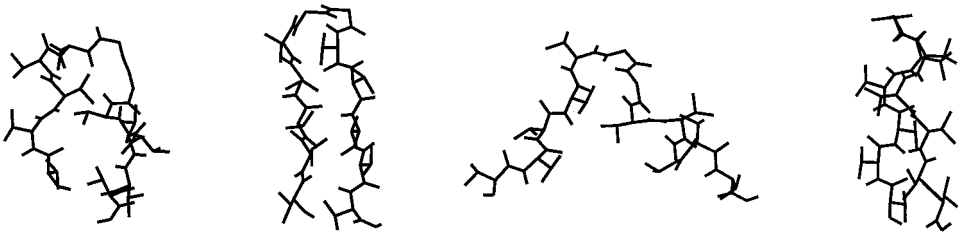

FIGURE 1 Selected conformations observed during simulation 1 with extended initial conformation and the solvation parameter of ±25 cal/mol/Å$^2$. From the left, the conformations are those at steps 9 M, 45 M, 86 M, and 200 M. In each conformation, the amino terminus of the peptide is on the left and the carboxy terminus is on the right. At step 9 M, a U-shaped conformation formed with the turn near the center of the molecule. At step 45 M, a β-hairpin formed, remaining stable for 40 M steps. The β-hairpin unfolded at step 86 M and refolded at step 90 M. The conformation at step 200 M shows the side chain packing and the right-handed twist in the β-hairpin conformation.

conformations, and several turns formed in various sites. At the GG site, type I′, type II, and type II′ turns formed and interconverted. The energy barrier between these types of turns did not prevent the conversion. At step 9 M, a U-shaped conformation formed with the turn near the center of the molecule. Although hydrogen bonds formed near the turn, they did not propagate to form a β-hairpin immediately. The adjustment of the orientations of the peptide units to form hydrogen bonds was relatively slow. At step 45 M, a β-hairpin formed, which was stable for the following 40 M steps. The β-hairpin unfolded at step 86 M and refolded 4 M steps later. During the rest of the simulation, the β-hairpin conformation unfolded and refolded several times. At step 200 M, the simulation was stopped and the conformation was a β-hairpin. During the simulation, the turn of the β-hairpin was mainly type II′ turns, although type I′ and type II were also observed.

In the β-hairpin conformation at step 200 M, the valine side chains were packed in pairs to reduce their exposure to the solvent and to lower the hydrophobic interaction energy. Both the hydrogen bonding and the hydrophobic interaction contribute to the stability of the β-hairpin structure. The conformation at step 200 M also showed the right-handed twist of the β-hairpin, which is consistent with experimental structures of β-sheet in proteins.

During the simulations, the conformation changed quickly, and a very large number of conformations occurred. It is not possible to show all these conformations. We use a simple graphic method to show when and where the β-hairpin occurred. Fig. 2 shows the locations and the simulation steps of the β-hairpin occurrence. These conformations were defined by the define secondary structure of protein (DSSP) algorithm (Kabsch and Sander, 1983). This algorithm is mainly based on hydrogen bonding patterns. A hydrogen bond is defined if its energy is lower than −0.5 kcal/mole, which allows the N-O distance up to 5.2 Å for perfect alignment of the H-N-O angle, and allows misalignment of the H-N-O angle up to 63° at the ideal N-O distance of 2.9 Å. With a hydrogen bond between the CO of residue $i$ and the NH of residue $i + n$, $n$-turns are defined for $n =$

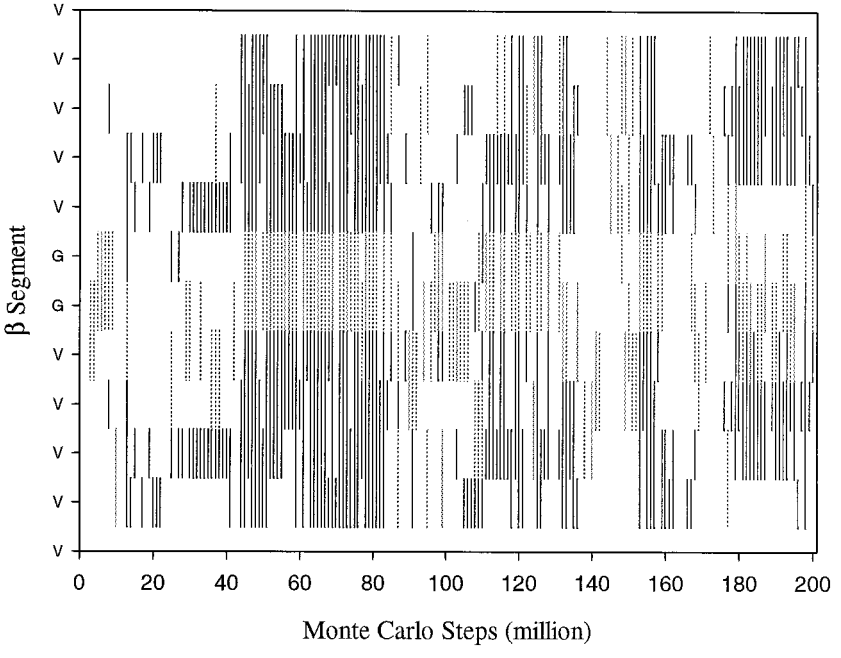


FIGURE 2 The locations of β-hairpin segments formed at different steps during simulation 1. The solid vertical lines represent the β-strands and the dotted vertical lines represent the turns. These structure elements are defined by the DSSP algorithm (Kabsch and Sander, 1983), as described in the text. The β-hairpin conformations are mainly concentrated in the periods approximately between steps 45 M and 84 M, 105 M and 115 M, 154 M and 158 M, and 179 M and 200 M.

3, 4, 5. Bridges are defined with the hydrogen bond between residues not near each other. Repeating turns form helices and repeating bridges form β-hairpins. The assignment of the β-hairpin segments in Fig. 2 is the result of the DSSP algorithm. The first and the last residues were not included in the conformation assignment. The average ratio of the β-hairpin conformation was ~37% for the whole simulation (200 M steps). Experimentally, isolated β-hairpin structures have the highest ratio below 50%. Therefore, the calculations showed a β-hairpin ratio comparable with experimental results. However, the model peptide does not have the same sequence as the experimental peptides, and the method of calculating the ratio is not the same as in the experimental measurement. Furthermore, the simulation is short and the average ratio fluctuated. Given these limitations, an accurate quantitative comparison is not possible in the current study.

The energy change during the simulation is shown in Fig. 3. Besides the initial relaxation, there is an energy decrease corresponding to the formation of the overall U-shaped structure at step 9 M. The U-shaped structure often contained hydrogen bonds. These hydrogen bonds were not in the correct pattern for a β-hairpin, but they contribute to lower energy. Corresponding to the β-hairpin conformations between steps 45 M and 84 M, the total energy is lower. The Coulomb interaction energy decrease is smaller than that of the total energy, indicating that the energy contribution of the hydrogen bonding to the β-hairpin structure is not large, but the hydrogen bonding is necessary for forming the ordered structure. Corresponding to the β-hairpin conformations, the hydrophobic interaction energy is lower. In the β-hairpin conformation in Fig. 1, the valine side chains are closely packed, which is favored by the hydrophobic interaction. The hydrophobic interaction favors the β-hairpin conformation. The formation of the hydrogen bonds between the backbone hydrophilic oxygen and nitrogen atoms contributes to a higher hydrophobic interaction energy. Therefore, the hydrophobic interaction energy decrease upon β-hairpin folding is only ~3 kcal/mol. The sharp Coulomb interaction energy drop between steps 171 M and 175 M corresponds to the formation of a transient α-helical segment between residues 1 and 11. This event showed that different secondary structures are accessible, and the β-hairpin conformation was not a result of the multiple minima problem, which prevents the formation of other structures.

A shorter peptide with 10 residues instead of 12, Ac-VVVVGGVVVV-$NH_2$, has also been tested with the same parameters as in simulation 1. With the extended initial conformation, stable β-hairpin conformations formed, but the turn was sometimes located at the VG or GV positions, instead of the GG position. Compared with simulation 1, the β-hairpin conformations of the 10-residue peptide seemed slightly less stable, but the basic features of the valine-based peptide folding into β-hairpins did not critically depend on small changes of the peptide size.

β-Hairpin folding has been successfully simulated from the extended initial conformation. However, experimentally observed folding is a statistical average of a large number of trajectories of many molecules. Although it is not possible to carry out as many simulations as those trajectories in a macroscopic experiment, multiple simulations from different initial conformations can make the study more reliable. Therefore, we carried out simulations with different initial conformations.

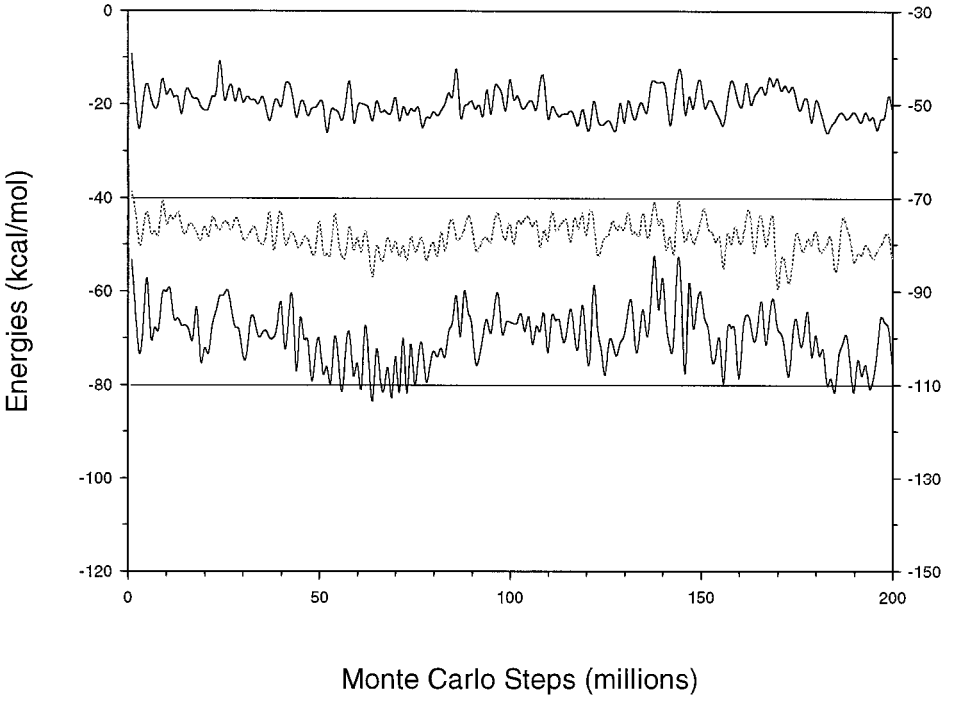


FIGURE 3 The energy changes during simulation 1. The energy scale on the left is for the hydrophobic interaction energy (the upper curve) and the total energy (the lower curve). The energy scale on the right is for the Coulomb interaction energy (the middle dotted curve). Corresponding to the β-hairpin conformation, between steps 45 M and 84 M and steps 180 M and 200 M, the hydrophobic interaction energy and the total energy are lower. The low Coulomb interaction energy at the period between steps 171 M and 175 M correspond to a transient helical segment between residues 1 and 11.

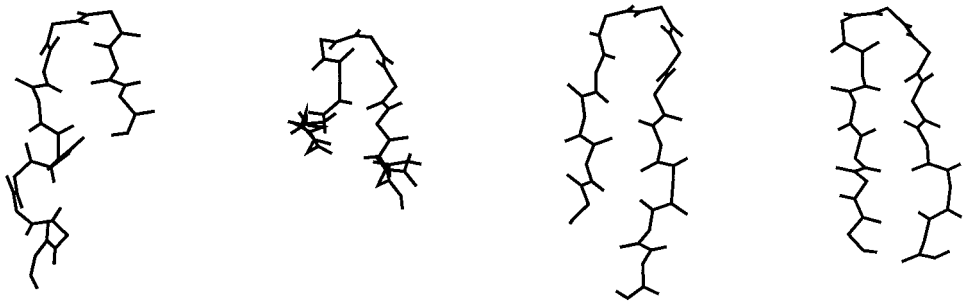

FIGURE 4 Selected conformations observed during simulation 2 with helical initial conformation and the solvation parameter of ±25 cal/mol/Å$^2$. From the left, the conformations are those at steps 20 M, 35 M, 60 M, and 66 M. The side chains are not shown. At step 20 M, a small β-hairpin occurred near the carboxy terminus and a short helical segment near the amino terminus. At step 35 M, a U-shaped conformation formed with two hydrogen bonds and unfolded at step 42 M. At step 60 M, a U-shaped conformation formed again. At step 66 M, a complete β-hairpin formed.

## Helical initial conformation

A helix has the maximal number of backbone hydrogen bonds and is the most stable structure for some sequences. Thus, a simulation (simulation 2 in Table 1) was carried out with an α-helical initial conformation. The temperature, dielectric constant, and solvation parameters remained the same as in the previous simulation. After the simulation started, the helix unfolded within the first 4 M steps. At approximately step 20 M, a small β-hairpin segment formed near the carboxy terminus with a turn at residues 9 and 10, whereas the amino terminus refolded into a helical segment, as shown in Fig. 4. At step 35 M, the whole molecule formed a U-shaped conformation, but the hydrogen bonds between the backbone of the two strands were not consistent with β-hairpin conformation. The carbonyl oxygen atoms of some consecutive residues were pointed in the same direction, instead of alternating directions as in the β-hairpin. The U-shaped conformation with incomplete hydrogen bonds occurred quite frequently. It often took a large number of steps, including unfolding and refolding of the U-shaped conformation, to convert to the β-hairpin hydrogen bonding pattern. The U-shaped conformation unfolded at step 42 M. At step 60 M, a U-shaped conformation formed again. At step 66 M, a complete β-hairpin formed. In the following steps, the β-hairpin conformation with frayed ends was largely preserved. At approximately step 190 M the whole β-hairpin unfolded. At the end of the simulation (step 200 M), the peptide refolded into a β-hairpin.

Fig. 5 shows the locations and the simulation steps of the β-hairpin occurrence. Compared with Fig. 2, the ratio of the β-hairpin in Fig. 5 seemed higher. Because the peptide sequence and all other parameters were the same in these two simulations, the average ratio should be the same during a long simulation, and the difference was a result of the structural fluctuation during the short simulation. The simulation contained only a single molecule, and therefore, the

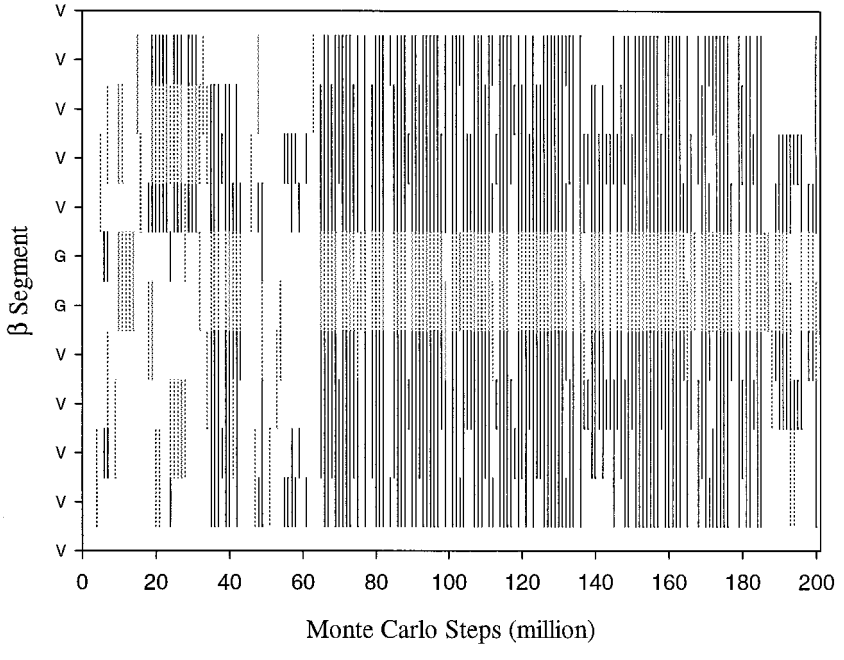


FIGURE 5 The locations of β-hairpin segments formed at different steps during simulation 2. The convention of this figure is the same as that of Fig. 2. The β-hairpin conformations occurred mainly in the periods between steps 66 M and 180 M.

fluctuation is quite pronounced. Our longest simulation ran for 800 M steps, and the fluctuation of the average ratio was still apparent at the end of that simulation. The experimentally observed macroscopic properties are usually the average properties of a large number of molecules (on the order of $10^{23}$) during a time period much longer than the simulations. Some aspect of the single molecule behavior in the simulation could deviate from the macroscopic behavior. For example, the experimentally observed folding time scale may be much longer than that in a simulation because a single molecule may fold and unfold many times before the average folding ratio reached a significantly different value.

The total energy of the $\beta$-hairpin conformations between steps 66 M and 180 M was lower than in the rest of the simulation, as shown in Fig. 6. The energy of the U-shaped conformations between steps 35 M and 42 M was also low. The hydrophobic interaction energy showed the same trend as the total energy. The Coulomb interaction energy of the initial helical conformation was low because the helix has the maximal number of hydrogen bonds. Why did the helix unfold and the $\beta$-hairpin form? The hydrophobic interaction, which has its origin in the solvent entropy, favors the $\beta$-hairpin conformation. Furthermore, a $\beta$-hairpin has fewer hydrogen bonds restraining the motion of the peptide and consequently may have larger conformational entropy than the helix.

## Different solvation parameters

For simplicity, only a single value of the solvation parameter was used. What about other values of the parameter? To answer this question, the solvation parameter $\pm 35$ cal/mol/Å$^2$ was tested to replace the $\pm 25$ cal/mol/Å$^2$ in a simulation (simulation 3 in Table 1). The temperature, the dielectric constant, and other parameters remained the same. The initial conformation is fully extended. The energy changes are shown in Fig. 7. As the simulation started, the structure relaxed and various coil conformations formed. Turns formed in various sites, including the GG site. With the larger solvation parameter, the peptide tended to stay longer in compact conformation with some backbone hydrogen bonds. The total energy was low between steps 110 M and 160 M, corresponding to a compact structure with low hydrophobic interaction energies, as shown in Fig. 7. A small transient $\beta$-hairpin occurred, but a stable $\beta$-hairpin was not observed during the first 200 M steps. At step 217 M, the whole molecule formed a U-shaped structure with the turn at the GG site and three hydrogen bonds between the two strands. From step 220 M to step 362 M, a $\beta$-hairpin occurred, but residues 2 and 3 were in the same orientation. These conformations had lower total energy than the compact conformations between steps 110 M and 160 M but higher hydrophobic interaction energy. At step 363 M, the orientation of the residues adjusted, and a complete $\beta$-hairpin formed and remained until the end of the simulation at step 400 M. The complete $\beta$-hairpin had lower total energy than the $\beta$-hairpin between steps 220 M and 362 M but higher hydrophobic interaction energy. During this simulation, the total energy was lowest for the complete $\beta$-hairpin conformation, the hydrophobic interaction energy was lowest for the compact conformation, as shown in Fig. 7. In this simulation, a similar folding process, including forming turns, U-shaped structures, and adjusting the residue orien-

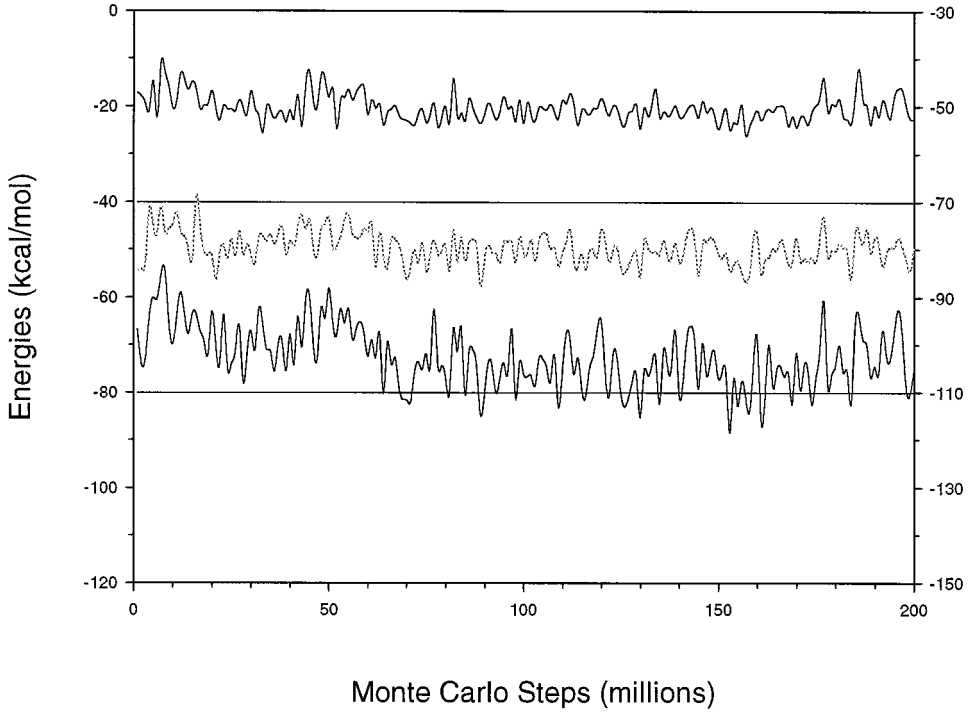


FIGURE 6 The energy changes during simulation 2. The convention of this figure is the same as that of Fig. 3. Corresponding to the U-shaped conformation between steps 35 M and 42 M and the $\beta$-hairpin between steps 66 M and 180 M, the hydrophobic interaction energy and the total energy are lower.

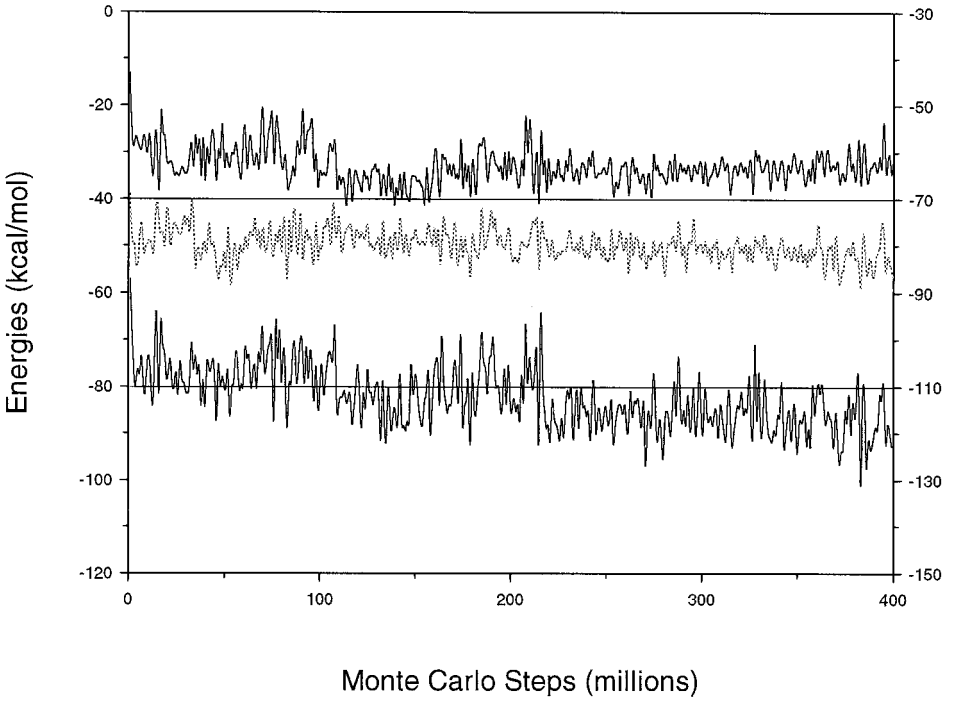


FIGURE 7 The energy changes during simulation 3 with extended initial conformation and the solvation parameter of $\pm 35$ cal/mol/Å$^2$. The convention of this figure is the same as that of Fig. 3. The total energy was low between steps 110 M and 160 M corresponding to a compact structure with low hydrophobic interaction energies. At step 217 M, the whole molecule formed a U-shaped structure. From step 220 M to step 400 M, an incomplete β-hairpin formed and rearranged into a complete β-hairpin. The total energy was low for the U-shaped conformations and the β-hairpin conformations.

tations, was observed as in simulation 1. However, the fluctuation in the hydrophobic interaction in Fig. 7 is larger than that in Fig. 3, indicating that the increased hydrophobic interaction caused a higher energy barrier for conformation changes. Therefore, folding into the β-hairpin took more steps than in simulation 1.

With solvation parameter $\pm 35$ cal/mol/Å$^2$, the helical initial conformation was also tested (simulation 4 in Table 1). The whole helix unfolded within the first 4 M steps. Some helical segments refolded later. At approximately step 70 M, a β-hairpin-like conformation formed, but residues 3 and 4 remained in the same orientation. Again, the adjustment of the orientation of the residues took many more steps before the peptide finally converted into a β-hairpin conformation. The tests with different solvation parameters showed that the β-hairpin folding simulation is not merely a fortunate coincidence of the chosen parameters. The qualitative results of the folding simulation showed relative stability with respect to small changes (40% increase from $\pm 25$ cal/mol/Å$^2$) of the solvation parameters.

During the several simulations of β-hairpin folding in the current study, the formation of a U-shaped conformation with a central turn is usually the first step and serves as the nucleation step. The subsequent formation of the rest of the hydrogen bonds in the β-hairpin pattern is the second step. The first step was analogous to the initial collapse in protein folding, with simultaneous nucleation. The ensemble of the U-shaped conformations with incomplete hydrogen bonds may be viewed as a folding intermediate, in analogy to the concept of the molten globule in protein folding. The second step of forming hydrogen bonds was slower than the formation of the U-shaped conformation. Because the major interaction in the β-hairpin is nonlocal, its folding resembled protein folding in some aspects. The β-hairpin structure was stabilized both by backbone hydrogen bonding and by side chain packing. Compared with helix, the hydrophobic effect was the major driving force for the β-hairpin formation. The role of the hydrogen bonding was to maintain the well ordered structure of the β-hairpin.

To see the limit of increasing the value of the solvation parameter in β-hairpin folding, the solvation parameter $\pm 47$ cal/mol/Å$^2$ was tested with the extended initial conformation (simulation 5 in Table 1). Before step 60 M, various turns formed at different sites. Occasionally, transient helix turns formed with fewer than four residues and unfolded quickly. At approximately step 60 M, a compact conformation formed with six or seven hydrogen bonds. This compact conformation contains several turns, and the amino terminus formed a hydrogen bond with the carboxy terminus. This compact conformation is very stable and did not undergo significant changes until the end of the simulation at step 200 M. The qualitative results of the folding simulation showed sensitivity to the larger changes (88% increase from $\pm 25$ cal/mol/Å$^2$) of the solvation parameters. However, this result comes as no surprise, because increasing any interaction beyond a limit will qualitatively change the simulation result. As there are more hydrophobic atoms than hydrophilic atoms in the peptide, the increased value of the solvation parameter caused the overall intramolecular interaction to become more attractive, instead of repulsive. The peptide becomes more compact, making conformation changes more difficult. The larger value of the solvation parameter caused a higher energy barrier, trapping the structure in a local minimal energy conformation. The value $\pm 47$ cal/mol/Å$^2$ does not work well with the parameters used in

the current study but may work well with other choices of the energy functions.

To further test the effect of different solvation parameters, a simulation (simulation 6 in Table 1) with zero solvation energy was carried out. This simulation has been run for 800 M steps, much longer than other simulations, but stable $\beta$-hairpin conformations did not form. Occasionally, short $\beta$-hairpin segments were observed, but they were often located near the termini (the turn is not at GG) and lasted fewer than 10 M steps. Occasional helical turns of three residues were observed but were not stable. This simulation showed that the solvation effect is crucial for $\beta$-hairpin folding, although the exact value of the solvation parameter may vary. It is likely that the difficulty for empirical force fields to simulate $\beta$-sheet folding arises mainly from the lack of the solvent effect.

## Distance dependence of the solvation effect

The specificity of the solvation interaction is different from that of the Coulomb interaction. The solvation interaction has a repulsive effect between two hydrophilic atoms and an attractive effect between two hydrophobic atoms, regardless of their charges. Besides this atom type specificity, the distance dependence of the interaction is also different from that of the Coulomb interaction. The surface-area-based calculation assumes the interaction range of one layer of water molecules (2.8 Å) beyond the VDW contact, but other contributions to solvation, such as electrostatic hydration, have longer interaction range. Therefore, we tested different interaction ranges of the solvation interaction. The interaction was extended to 5.6 Å beyond the VDW contact of two atoms; i.e., the interaction energy decreased more slowly as the interatomic distance increased. The simulation (simulation 7 in Table 1) started with an extended initial conformation. At step 63 M, a $\beta$-hairpin conformation with three hydrogen bonds formed. The turn was in the center of the peptide, and the ends of the two strands were frayed. A complete $\beta$-hairpin conformation formed at step 125 M and was stable to the end of the simulation at step 200 M. During this simulation the hydrophobic interaction energy was lower than in the previous simulations, because the longer interaction range increased the number of hydrophobic interaction pairs. This example showed that the $\beta$-hairpin folding simulation is not limited to the frame of the surface-area-based solvation.

Because the hydrophilic interaction has its major contribution from electrostatic hydration, an $r^{-4}$ distance dependence (Gilson and Honig, 1991) has been tested within a 15-Å interaction range for the hydrophilic atoms O and N (simulation 8 in Table 1). With extended initial conformation, stable $\beta$-hairpins formed during the simulation. Many $\beta$-hairpin conformations occurred and interconverted. Sometimes, the turn was not at the GG site. Three-residue turns were also observed. The qualitative feature of folding was similar to that in simulation 1 and was not very sensitive to the distance dependence of the interaction. The specificity of the atom types in the hydrophobic interaction is more important than the distance dependence of the interaction. Although the exact distance dependence is currently not known, it is not very restrictive for approximate calculations.

## Different dielectric constant

Different values of the dielectric constant have been tested. First, a simulation with dielectric constant 3 was carried out (simulation 9 in Table 1). All other parameters remained the same as in simulation 1. A short $\beta$-hairpin conformation with three hydrogen bonds formed before step 40 M and unfolded in 3 M steps. At steps 55 M, 78 M, and 152 M, short $\beta$-hairpin conformations formed again at different sites. These $\beta$-hairpin conformations usually last for 3 M to 5 M steps. Between steps 194 M and 200 M, a $\beta$-hairpin occurred with four hydrogen bonds and a central turn at the GG. With the weaker Coulomb interaction, the $\beta$-hairpin conformations were less stable than with dielectric constant 2 in simulation 1.

Dielectric constant 4 has also been tested (simulation 10 in Table 1) with all other parameters remaining the same as in simulation 1. Occasionally, short $\beta$-hairpins formed with two to four hydrogen bonds, but they were not stable and lasted for fewer than 4 M steps. No stable structures were observed during the 200 M step simulation.

As mentioned previously, using dielectric constant 1 without solvent overestimates the Coulomb interaction. In our tests with dielectric constant 1, three simulations with different initial conformations were carried out (all three simulations are included in Table 1 as simulation 11). Depending on the initial conformation, the peptide formed different stable structures early in the simulation and remained largely unchanged until the end of the simulation. Starting with an extended initial conformation, a helix-turn-helix type of conformation formed with the turn in the GG position. Instead of forming $\beta$-strands, the valine residues formed two residue strands near the turn and the distorted helix turns near the ends of the peptide. Starting with a helical structure, the peptide remained in helical conformation, except for the end residues, which unfolded and refolded during the simulation. Starting with a $\beta$-hairpin, the peptide remained in the $\beta$-hairpin conformation. In all three cases, the structure remained in the local energy minimum near the initial conformation. With dielectric constant 1, the simulation suffered from the multiple minima problem because the energy landscape of folding contains deep local energy minima (compared with the global minimum).

An interesting conclusion may be drawn from the tests of dielectric constant 1. Because an overestimated interaction can prevent conformational changes from the initial conformation, the ability to maintain a crystal structure in a simulation alone does not justify a force field. If a force field can maintain the crystal structure, after uniformly

scaling up the interactions by a factor of 10, the new force field should also keep the conformation near the initial structure. The original force field and the new force field can both maintain a crystal structure, but they cannot both be justified, if the interaction strength has an objective magnitude in reality. In this case, a smaller root mean square deviation from the crystal structure does not mean a better force field.

It is clear that with an overestimated interaction, such as using dielectric constant 1 without solvent, the multiple energy minima will prevent correct folding, and with an underestimated interaction, such as using dielectric constant 4, the structure will not be stable. The question is whether there is an intermediate region for the simple form of the energy function to model folding at a constant temperature. Our simulation results showed the existence of such a region; i.e., the simple energy function can model peptide folding. The tests on the solvation parameters showed a similar situation. The solvation parameter $\pm 47$ cal/mol/Å$^2$ made the attractive interaction too strong for folding. The zero solvation made the attractive interaction too weak to have stable structures. The $\pm 25$ cal/mol/Å$^2$ and $\pm 35$ cal/mol/Å$^2$ correspond to the proper range for folding.

In MC simulations, scaling up the interaction energy has a similar effect to lowering temperature. An analogy could be drawn between the folding simulation with different energy functions and the structural transition under varying temperatures, such as the glass transition (Bryngelson and Wolynes, 1987; Goldstein et al., 1992; Socci and Onuchic, 1994; Dill et al., 1995). When the temperature is high, a glass fluid does not have a stable configuration, which is analogous to the unstable structures of peptides in the simulation with an underestimated interaction. As the temperature decreased to below the glass transition temperature, the glass fluid forms disordered structures, which is analogous to the peptide conformations trapped at local energy minima with an overestimated interaction. The glass transition does not have an intermediate temperature range to form a unique structure. In contrast, protein folding has an intermediate range of experimental conditions to form a unique structure. A difficult task in computational study of protein folding is to find a proper energy function that can lead to a unique structure, instead of the glass transition. Our simulations showed that the simple energy function modified to include solvent effect has a parameter range that can simulate secondary structure folding at constant temperature. A range of energy function parameters, instead of a single value, makes further refinement of the energy function possible to differentiate more detailed structure features.

## Alanine-based peptide

It is important to show that the method (mainly the energy function) does not fold every sequence into a β-hairpin structure. Therefore, the alanine-based synthetic peptide Ac-$(AAQAA)_3$Y-$NH_2$ was simulated (simulation 12 in Table 1) with the same energy function as in simulation 1. The initial conformation was fully extended. During the simulation, a helix turn first formed near the carboxy terminus between residues 11 and 14, which represented the nucleation of helix folding. Instead of quickly propagating to the whole molecule, the helix segment propagated to residue 9 and paused. Then, another helix turn formed near the amino terminus between residues 1 and 3, which may be considered as the second nucleation at a different site. At step 7 M, the two helical segments formed a complete helix. Similar helix folding has been observed and reported in detail in previous studies (Sung, 1994, 1995; Sung and Wu, 1996, 1997).

It is interesting to compare helix folding with β-hairpin folding. Table 2 shows the energy changes per residue estimated from simulations 1, 2, and 12, which were carried out with the solvation parameter $\pm 25$ cal/mol/Å$^2$ and the dielectric constant 2. In simulations 1 and 2 the folded conformations are β-hairpins, and in simulation 12 the folded conformations are α-helices. These values in Table 2 are differences of the average energies between the samples of different structure types. Depending on the conformations in the samples, the average energies may vary. For example, the helical structure may include conformations with partially unfolded helices, and the coil structure may include small helical segments. Because most conformations in the simulation do not have the ideal geometry of a specific structure type, it is difficult to make a practical criterion for each type of structure. Also, because the numbers of conformations are quite limited in the simulations, the values in Table 2 represent only a qualitative estimate. For simulation 1, the average energies of the β-hairpin, the

**TABLE 2 Estimated energy changes upon β-hairpin and α-helix folding**

| | $E_{fold}$–$E_{coil}$ | | | $E_{fold}$–$E_{compact}$ | | |
|---|---|---|---|---|---|---|
| Simulation | Total | Coulomb | Solvation | Total | Coulomb | Solvation |
| 1 | −1.0 | −0.3 | −0.3 | −0.8 | −0.4 | −0.3 |
| 2 | −1.0 | −0.5 | −0.3 | −0.5 | 0.0 | −0.1 |
| 12 | −1.3 | −1.0 | −0.2 | (−0.4) | (−0.4) | (+0.3) |

This table shows the energy changes per residue, including the total energy, the Coulomb energy, and the solvation (or hydrophobic interaction) energy, estimated from simulations with the solvation parameter $\pm 25$ cal/mol/Å$^2$ and the dielectric constant 2. In simulations 1 and 2 the folded conformations are β-hairpins, and in simulation 12 the folded conformations are α-helices. The values in the parentheses are from other helix-folding simulations because the typical compact conformations were not found in simulation 12.

extended coil, and other compact structures (including some U-shaped conformations) are calculated from the time periods between steps 45 M and 84 M, 140 M and 149 M, and 9 M and 44 M, respectively. For simulation 2, the average energies of the $\beta$-hairpin, the extended coil, and other compact structures are calculated from the time periods between steps 66 M and 180 M, 42 M and 46 M, and 20 M and 28 M, respectively. The differences between the results of simulations 1 and 2 show the dependence of the energies on the conformations sampled. For example, the compact structures in simulation 1 are quite different from those in simulation 2. For simulation 12, the average energies of the $\alpha$-helix are calculated from the time period between steps 7 M and 200 M, those of the extended coil between steps 1 M and 4 M. Typical compact structures were not found in simulation 12. The energy differences between the helix and the compact structure (the values in the parentheses) are calculated using structures sampled from another helix folding simulation in which the compact structure (including the helix-turn-helix conformation) occurred for more than 10 M steps.

Upon helix folding, the Coulomb interaction energy decreases sharply because a helix has the maximal number of hydrogen bonds (the $3_{10}$ helix has one more hydrogen bond than an $\alpha$-helix). In contrast, upon $\beta$-hairpin folding, the Coulomb interaction energy decreased less because there are fewer hydrogen bonds. Also, the hydrogen bonds of a helix are usually more stable, with shorter O-H distance and longer lifetime than those in a $\beta$-hairpin. The Coulomb energy is closely related to the hydrogen bonds, but it includes the interactions between non-hydrogen-bonded atom pairs as well. Also, the hydrogen bond energy includes the increase in solvation energy as the hydrophilic atoms O and N approach each other. When a helix folds, the total solvation energy decreases compared with the extended coil conformations, as other studies indicated (Yang and Honig, 1995). Compared with other compact conformations, the solvation energy may increase because some hydrophobic surfaces become more exposed and hydrophilic surface less exposed (Sung and Wu, 1996). In contrast, when a $\beta$-hairpin folds, the hydrophobic energy decreases (with $\pm$25 cal/mol/Å$^2$), compared with both the extended coil and other compact structures. These energy changes may indicate that hydrogen bonds contribute more to the stability of the helix, and the hydrophobic interaction is more crucial for $\beta$-hairpin conformations. The smaller total energy change upon $\beta$-hairpin folding may explain why the $\beta$-hairpin structure is less stable than the $\alpha$-helix for small peptides (Alba et al., 1995, 1997; Blanco et al., 1993, 1994; Ramirez-Alvarado et al., 1996).

## CONCLUSION

This study demonstrated the following. 1) A simple model including an approximate average solvent effect can simulate the qualitative feature of the secondary structure folding. Depending on the amino acid sequence, this model can differentiate not only between stable structures and random coils but also between $\alpha$-helix and $\beta$-hairpin. 2) This approach reduces the exaggerated interactions of the empirical force field without solvent effects. Consistent with the fact that proteins fold into stable structures, a range of the simple energy function exists between those exaggerated potentials trapping the structure in local minima and those underestimated potentials destabilizing the structure. Further testing on more peptide structures will narrow down the range and uncertainty of the energy function and eventually reach the limits of this approach. Once the sufficient computing power and a proven force field for folding become available, the folding simulation with explicit water molecules will be the method of choice. Until then, simple models can still provide information relevant to folding.

The simulations provided insights into the $\beta$-hairpin folding mechanism. Driven by the hydrophobic interaction, the whole peptide folded into a compact U-shaped conformation with a central $\beta$-turn. This step may resemble the initial collapse and nucleation (the central $\beta$-turn) in protein folding. Hydrogen bonds of the $\beta$-hairpin pattern formed afterwards as the peptide units reoriented. The reorientation of the residues was relatively slow and resembled the transition from a molten globule state to the native state of proteins. The hydrogen bonds often formed first in the $\beta$-turn and then propagated along the strands toward the termini. The hydrophobic interaction included in the simulation played a crucial role in $\beta$-hairpin folding. The difficulty for empirical force fields to simulate $\beta$-sheet folding may arise mainly from the lack of the solvent effect.

The author thanks Dr. George D. Rose for suggesting the valine-based amino acid sequence for folding simulations and Dr. Hongwu Wang for helping to prepare some of the figures.

## REFERENCES

Alba, E., F. J. Blanco, M. A. Jimenez, M. Rico, and J. L. Nieto. 1995. Interactions responsible for the pH dependence of the $\beta$-hairpin conformational population formed by a designed linear peptide. *Eur. J. Biochem.* 233:283–292.

Alba, E., M. A. Jimenez, and M. Rico. 1997. Turn residue sequence determines $\beta$-hairpin conformation in designed peptide. *J. Am. Chem. Soc.* 119:175–183.

Blanco, F. J., M. A. Jimenez, J. Herranz, M. Rico, J. Santoro, and J. L. Nieto. 1993. NMR evidence of a short linear peptide that folds into a $\beta$-hairpin in aqueous solution. *J. Am. Chem. Soc.* 115:5887–5888.

Blanco, F. J., J. Rivas, and L. Serrano. 1994. A short linear peptide that folds into a native stable $\beta$-hairpin in aqueous solution. *Struct. Biol.* 1:584–590.

Bryngelson, J. D., and P. G. Wolynes, 1987. Spin glasses and the statistical mechanics of protein folding. *Proc. Natl. Acad. Sci. U.S.A.* 84: 7524–728.

Chakrabartty, A., T. Kortemme, and R. L. Baldwin. 1994. Helix propensities of the amino acids measured in alanine-based peptides without helix-stabilizing side-chain interactions. *Protein Sci.* 3:843–852.

Chandler, D., J. D. Weeks, and H. C. Andersen. 1983. Van der Waals picture of liquids, solids, and phase transformations. *Science*. 220: 787–794.

Chothia, C. 1974. Hydrophobic bonding and accessible surface area in proteins. *Nature*. 248:338–339.

Chou, P. Y., and G. D. Fasman. 1973. Structural and functional role of leucine residues in proteins. *J. Mol. Biol.* 74:263–281.

Chou, P. Y., and G. D. Fasman. 1974. Conformational parameters for amino acids in helical, beta-sheet, and random coil regions calculated from proteins. *Biochemistry*. 13:211–222.

Colonna-Cesari, F., and C. Sander. 1990. Excluded volume approximation to protein-solvent interaction: the solvent contact model. *Biophys. J.* 57:1103–1107.

Daggett, V., P. A. Kollman, and I. D. Kuntz. 1991. Molecular dynamics simulations of small peptides: dependence on dielectric model and pH. *Biopolymers*. 31:285–304.

Daggett, V., and M. Levitt. 1992. Molecular dynamics simulations of helix denaturation. *J. Mol. Biol.* 223:1121–1138.

Daura, X., B. Jaun, D. Seebach, W. F. van Gunsteren, and A. E. Mark. 1998. Reversible peptide folding in solution by molecular dynamics simulation. *J. Mol. Biol.* 280:925–932.

Dill, K. A. 1985. Theory for the folding and stability of globular proteins. *Biochemistry*. 24:1501–1509.

Dill, K. A., S. Bromberg, K. Yue, K. M. Fiebig, D. P. Yee, P. D. Thomas, and H. S. Chan. 1995. Principles of protein folding: a perspective from simple exact models. *Protein Sci.* 4:561–602.

Eisenberg, D., and A. D. McLachlan. 1986. Solvation energy in protein folding and binding. *Nature*. 319:199–203.

Finkelstein, A. V. 1997. Can protein unfolding simulate protein folding? *Protein Eng.* 10:843–845.

Gilson, M. K., and B. Honig. 1991. The inclusion of electrostatic hydration energies in molecular mechanics calculations. *J. Comput. Aided Mol. Des.* 5:5–20.

Goldstein, R. A., Z. A. Luthey-Schulten, and P. G. Wolynes. 1992. Optimal protein folding codes from spin-glass theory. *Proc. Natl. Acad. Sci. U.S.A.* 89:4918–4922.

Kabsch, W., and C. Sander. 1983. Dictionary of protein secondary structure: pattern recognition of hydrogen-bonded and geometrical features. *Biopolymers.* 22:2577–2637.

Kortemme, T., Ramirez-Alvarado, and L. Serrano. 1998. Design of a 20-amino acid, three-stranded β-sheet protein. *Science*. 281:253–256.

Kurochkina, N., and B. Lee. 1995. Hydrophobic potential by pairwise surface area sum. *Protein Eng.* 8:437–442.

Lee, B., and F. M. Richards. 1971. The interpretation of protein structures: estimation of static accessibility. *J. Mol. Biol.* 55:379–400.

McCammon, J. A., S. H. Northrup, M. Karplus, and R. M. Levy. 1980. Helix-coil transitions in a simple polypeptide model. *Biopolymers*. 19: 2033–2045.

Miyazawa, S., and R. L. Jernigan. 1985. Estimation of effective interresidue contact energies from protein crystal structures: quasi-chemical approximation. *Macromolecules*. 18:534–552.

Momany, F. A., R. F. McGuire, A. W. Burgess, and H. A. Scheraga. 1975. Energy parameters in polypeptides. VII. Geometric parameters, partial atomic charges, nonbonded interactions, hydrogen bond interactions, and intrinsic torsional potentials for the naturally occurring amino acids. *J. Phys. Chem.* 79:2361–2381.

Okamoto, Y. 1998. Protein folding problem studied by new simulation algorithms. *Dev. Pure Appl. Chem.* 2:1–23.

Okamoto, Y., M. Fukugita, T. Nakazawa, and H. Kawai. 1991. Alpha-helix folding by Monte Carlo simulated annealing in isolated C-peptide of ribonuclease A. *Protein Eng.* 4:639–647.

Ooi, T., and M. Oobatake. 1991. Prediction of the thermodynamics of protein unfolding: the helix-coil transition of poly(L-alanine). *Proc. Natl. Acad. Sci. U.S.A.* 88:2859–2863.

Ramirez-Alvarado, M., F. J. Blanco, and L. Serrano. 1996. De novo design and structural analysis of a model β-hairpin peptide system. *Nature Struct. Biol.* 3:604–612.

Ripoll, D. R., and H. A. Scheraga. 1988. On the multiple-minima problem in the conformational analysis of polypeptides. II. An electrostatically driven Monte Carlo method: tests on poly(L-alanine). *Biopolymers*. 27:1283–1303.

Schaefer, M., and M. Karplus. 1995. A comprehensive analytical treatment of continuum electrostatics. *J. Chem. Phys.* 100:1578–1599.

Schenck, H. D., and S. H. Gellman. 1998. Use of a designed triple-stranded antiparallel β-sheet to probe β-sheet cooperativity in aqueous solution. *J. Am. Chem. Soc.* 120:4869–4870.

Scholtz, J. M., E. J. York, J. M. Stewart, and R. L. Baldwin. 1991. A neutral, water-soluble, α-helical peptide: the effect of ionic strength on the helix-coil equilibrium. *J. Am. Chem. Soc.* 113:5102–5104.

Shakhnovich, E. I., and A. M. Gutin. 1991. Influence of point mutations on protein structure: probability of a neutral mutation. *J. Theor. Biol.* 149:537–546.

Sharp, K. A., A. Nicholls, R. Friedman, and B. Honig. 1991. Extracting hydrophobic free energies from experimental data: relationship to protein folding and theoretical models. *Biochemistry*. 30:9686–9697.

Skolnick, J., and A. Kolinski. 1990. Simulations of the folding of a globular protein. *Science*. 250:1121–1125.

Socci, N. D., and J. N. Onuchic. 1994. Folding kinetics of protein-like heteropolymers. *J. Chem. Phys.* 100:1519–1528.

Sung, S. S. 1994. Helix folding simulations with various initial conformations. *Biophys. J.* 66:1796–1803.

Sung, S. S. 1995. Folding simulations of alanine-based peptides with lysine residues. *Biophys. J.* 68:826–834.

Sung, S. S., and X. W. Wu. 1996. Molecular dynamics simulations of synthetic peptide folding. *Proteins.* 25:202–214.

Sung, S., and X. W. Wu. 1997. Molecular dynamics simulations of helix folding: the effects of amino acid substitution. *Biopolymers*. 42: 633–644.

Taketomi, H., Y. Ueda, and N. Go. 1975. Studies on protein folding, unfolding and fluctuations by computer simulation. I. The effect of specific amino acid sequence represented by specific inter-unit interactions. *Int. J. Pept. Protein Res.* 7:445–459.

Weiner, S. J., P. A. Kollman, D. A. Case, U. C. Singh, C. Ghio, G. Alagona, S. Profeta, Jr., and P. Weiner. 1984. A new force field for molecular mechanical simulation of nucleic acids and proteins. *J. Am. Chem. Soc.* 106:765–784.

Wojcik, J., K. H. Altmann, and H. Scheraga. 1990. Helix-coil stability constant for the naturally occurring amino acids in water. XXIV. Half-cysteine parameters from random poly(hydroxybutylglutamine-co-S-methylthio-l-cysteine). *Biopolymers*. 30:121–134.

Yang, A.-S., and B. Honig. 1995. Free energy determinants of secondary structure formation: I. α-Helices. *J. Mol. Biol.* 252:351–365.